THE JOURNAL OF PHYSICAL CHEMISTRY B

Article

pubs.acs.org/JPCB

Reversible Polymerization in Doped Fullerides Under Pressure: The Case Of $C_{60}(Fe(C_5H_5)_2)_2$

Wen Cui, Mingguang Yao, Dedi Liu, Quanjun Li, Ran Liu, Bo Zou, Tian Cui, and Bingbing Liu*

State Key Laboratory of Superhard Materials, Jilin University, Changchun 130012, China

ABSTRACT: High-pressure Raman studies have been carried out on single crystalline $C_{60}(Fc)_2$ nanosheets up to 25.4 GPa. Our results show that the charge transfer between Fc (ferrocene) and C_{60} increases in the low-pressure range. Above 5 GPa, C_{60} molecules start to form a chainlike polymer structure, and this polymerization is reversible upon decompression, in contrast to that of pristine C_{60}. The special layered structure of $C_{60}(Fc)_2$ restricts the polymerization of C_{60} molecules in some directions and explains the formation of the linear chainlike polymeric structure of the C_{60} lattice under pressure. We suggest that the reversible polymerization is related to the increased charge transfer and the overridden steric repulsion of counterions.

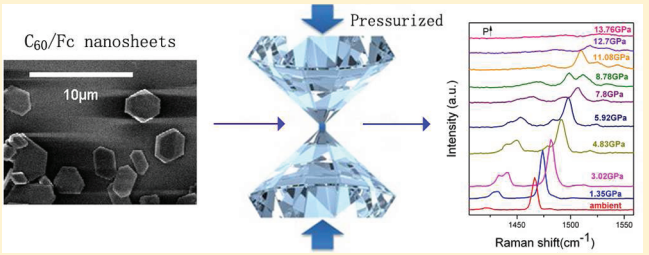

1. INTRODUCTION

The doping of fullerenes C_{60} with various species, such as alkali metals, p-elements such as oxygen, nitrogen, and sulfur, organometallic donors, etc., have attracted great interest because of the resulting unique structures and extraordinary physical properties.[1−6] For example, alkali-metal-intercalated fullerides[1] show semiconducting, metallic, or even superconducting properties, and the fullerene molecules either remain in monomer form with weak interactions or form covalently bonded polymerized phases with one- or two-dimensional structures, depending on the charge transfer to C_{60} and the size of the metal ions. S-doped C_{60} compounds[2] form layered structures with weak van der Waals interaction. Furthermore, C_{60} can form a wide variety of donor−acceptor complexes with organometallic donors. These show various properties, such as metallic, photoconducting, and unusual magnetic properties.[3,7,8] Such complexes are formed due to the relatively weak van der Waals interactions and the effects of charge transfer from donors to acceptors.[9] However, some studies show that the degree of charge transfer is very small between C_{60} molecules and dopants even if the dopants have a strong electron-donating ability. Thus, it has not been understood why these strong electron donors are unable to donate electrons to the C_{60} molecules. To understand this phenomenon is also important for tuning the properties of the intercalated fullerides and thus for their potential applications. Ferrocene (Fc, $Fe(C_5H_5)_2$) is an example of a material which has a strong electron-donating ability but gives weak charger transfer to C_{60},[10] and studies of Fc−C_{60} compounds thus provide good opportunities to study how to tune the degree of charge transfer between C_{60} and strong electron-donating dopants. It has been also reported that the degree of charge transfer in the donor−acceptor complexes is mainly determined by the vertical ionization potentials of donors and the electron affinity of acceptors together with the efficiency of the HOMO (the highest occupied molecular orbital)−LUMO (the lowest unoccupied molecular orbital) overlap which is related to the distance between donors and acceptors.[9] High-pressure methods have recently been widely used in different fields[11−13] as an efficient method to change (shorten) the intermolecular distance and thus affect the charge transfer between host and guest. It may be expected that the interaction between C_{60} and Fc molecules can be tuned by applying pressure, but only few studies have been carried out on this topic in organometal-doped C_{60} materials, and the corresponding mechanism transferring charge under pressure in this system is still unclear and worth studying.

Pristine C_{60} can also be polymerized into one-dimensional (1D), two-dimensional (2D), and even three-dimensional (3D) structures by high-temperature and high-pressure treatment.[14−17] However, C_{60} does not form well-ordered polymers but transforms to an amorphous (probably disordered polymer) structure when treated by cold compression.[18] Much effort has been made to produce polymeric fullerene structures at ambient temperature. Recently, the intercalation with alkali metals and with p-elements such as oxygen, nitrogen, and sulfur has been found to be a possible way to favor the polymerization of C_{60}. For example, Na_4C_{60}[19] has a strong charge transfer interaction between fullerene and dopants and forms a unique 2D polymeric structure, in which each fullerene molecule is linked to four other neighbors by single covalent C−C bonds in a plane. A reversible orthorhombic polymerization has also been observed in Na_2RbC_{60} and Na_2CsC_{60}[20] due to the overridden steric repulsion of the counterions under pressure at room temperature. Compressing the S-doped fullerene ($C_{60}S_{16}$)[21] results in C_{60} polymerization with a better

Received: November 8, 2011
Revised: January 14, 2012
Published: February 14, 2012

ordered structure due to the initially layered structure and the formation of C−S−C bridges. Thus, the doped C_{60} compounds show polymerization mechanisms that differ from those of pure C_{60} under pressure due to the presence of charge transfer between C_{60} and dopants. Understanding how the charge transfer affects the polymerization is important for the development of a controllable way to synthesize desired polymeric structures of fullerenes.

The possibility to tune the polymerization in fullerenes by changing the doping species and the high-pressure techniques make such weak charge transfer donor−acceptor complexes interesting systems. Such high-pressure studies on intercalated fullerene compounds may also be expected to produce completely new materials.

As an important and typical organometal-doped C_{60} material, $C_{60}(Fc)_2$, is expected to comply with this topic. In this work, single crystalline $C_{60}(Fc)_2$ nanosheets with a triclinic lattice structure are successfully fabricated by introducing Fc into a saturated C_{60}/toluene solution. We report in situ high-pressure Raman results on the sample up to 25.4 GPa, showing that $C_{60}(Fc)_2$ polymerizes at about 5 GPa and that the polymerization is reversible upon decompression. Further discussions concerning the possible polymerization mechanisms have been carried out considering pressure-tuned changes in the charge transfer compounds and the unique special layered structure of C_{60}/Fc.

2. EXPERIMENTAL METHOD

The single crystalline $C_{60}(Fc)_2$ nanosheets were prepared by introducing 200 mg of Fc into 3 mL of saturated C_{60}/toluene solution. After ultrasonication we then added 3 mL of isopropyl alcohol (IPA), and the mixture was maintained at 10 °C for 24 h for the growth of single crystalline $C_{60}(Fc)_2$ nanosheets. The morphologies of the obtained as-grown samples were characterized by scanning electron microscopy (SEM, JEOL JSM-6700F), X-ray diffraction (Rigaku D/max-RA, CuKα1 radiations λ = 1.5406 Å), and thermogravimetry analysis (TGA). The TGA measurement was performed at a 10 °C min^{-1} heating rate under nitrogen atmosphere.

For high-pressure studies, samples were loaded into a 140 μm diameter hole in a T301 stainless steel gasket. Silicone oil was used as pressure medium. In situ high-pressure Raman measurements have been carried out at room temperature using a Raman spectrometer (Renishaw in Via) with a 514.5 nm Ar^+ laser line as excitation. The highest pressure reached in this study is 25.4 GPa.

3. RESULTS AND DISCUSSION

A representative SEM image of as-grown nanosheets is shown in Figure 1. From this figure we can see that the nanosheets have a hexagonal morphology. The average size of the nanosheets is from 3 to 6 μm (see Figure 1a), and the thickness is in the range of 250−500 nm (Figure 1b). The XRD pattern and the TGA curve from the $C_{60}(Fc)_2$ nanosheets samples are shown in parts a and b of Figure 2, respectively. The XRD pattern of the sample identifies the structure of $C_{60}(Fc)_2$ as triclinic, which is consistent with the previous report by Espeau et al.[22] The TGA curve shows that there are two steps of weight loss in the temperature range studied. The first step starts at 110 °C and gives 34% weight loss, indentified as the evaporation of Fc molecules, indicating that the mole ratio of C_{60} and Fc molecules is 2:1.

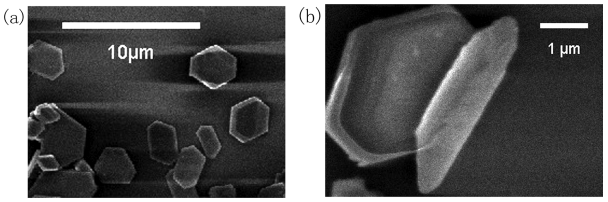

Figure 1. SEM images of $C_{60}(Fc)_2$ at low (a) and high (b) magnification.

Raman spectroscopy is a powerful tool to characterize C_{60} and C_{60}-based materials. The Raman spectra of C_{60} $(Fc)_2$ at different pressures are shown in Figure 3. At ambient condition, the line at 267 cm^{-1} corresponds to the Hg(1) intramolecular mode in pristine C_{60}. Compared with pure C_{60}, this mode displays an obvious shoulder. A similar splitting in this Hg mode has already been reported in alkali-metal-doped C_{60} and was attributed to a charge transfer interaction.[23] The Ag(1) radial breathing intramolecular mode is observed at 490 cm^{-1}. The peak at 1422 cm^{-1} is the Hg(7) intramolecular mode. The line at 1467 cm^{-1} is attributed to the tangential double-bond stretching pentagon pinch Ag(2) intramolecular mode. In addition to the peaks from C_{60}, there are also two peaks with positions at 317 and 1105 cm^{-1} which represent the vibrational modes from the inserted Fc molecules. Here we denote the two peaks as Fc(1) and Fc(2), respectively.

As the pressure increases, some peaks become broader and weaker. From Figure 3, we can see that the Hg(1) mode clearly splits with increasing pressure. As pointed out above, this mode already shows a shoulder at ambient pressure possibly due to the weak charge transfer.[23] Also, the Hg(7) mode starts to show a shoulder at above 1.4 GPa and exhibits an obvious splitting from above 3 GPa. Up to 8.8 GPa, these two peaks merge into one broad peak. Furthermore, we observed an obvious change in the nondegenerate Ag modes. The Ag(2) mode displays a splitting, with a shoulder appearing at 1478 cm^{-1} at around 4.8 GPa. It should be noted that the two peaks shift to higher frequency with a constant frequency difference of 12−13 cm^{-1} as the pressure increases. Both peaks can be observed up to 13.8 GPa. Also, some new Raman peaks can be observed around 600−800 cm^{-1}, and a broad peak around 900−1000 cm^{-1} is growing with increasing pressure. All these changes indicate the occurrence of some transitions in the material, and they will be discussed later. Besides the changes in the Raman modes of C_{60}, we also find that the two modes from the Fc molecules disappear with increasing pressures. We further analyze the pressure dependence of these modes in Figure 4, and the numerical values of the slopes for Raman shift versus pressure are shown in Table 1. Figure 4 shows that an obvious change in the slopes of the pressure dependence of the Hg(1), Fc(1), and Fc(2) modes is observed at 1−2 GPa. At this pressure, the Hg(7) mode also shows an obvious splitting. At 5 GPa, the Ag(2) mode starts to display an obvious splitting, while the Ag(1) mode exhibits a change in the slope for Raman shift versus pressure at around 4 GPa.

The anomalies observed in the Raman spectra can be interpreted in terms of structural phase transitions in the material. The first transition set of anomalies observed in the Raman spectra of the sample consists of changes in the slopes of the pressure dependence of Hg(1), Fc(1), and Fc(2) at about 1 GPa, and a splitting of the Hg(7) mode. Such a change in slope for the Hg(1) mode could possibly relate to the phase

dx.doi.org/10.1021/jp210712y | J. Phys. Chem. B 2012, 116, 2643−2650

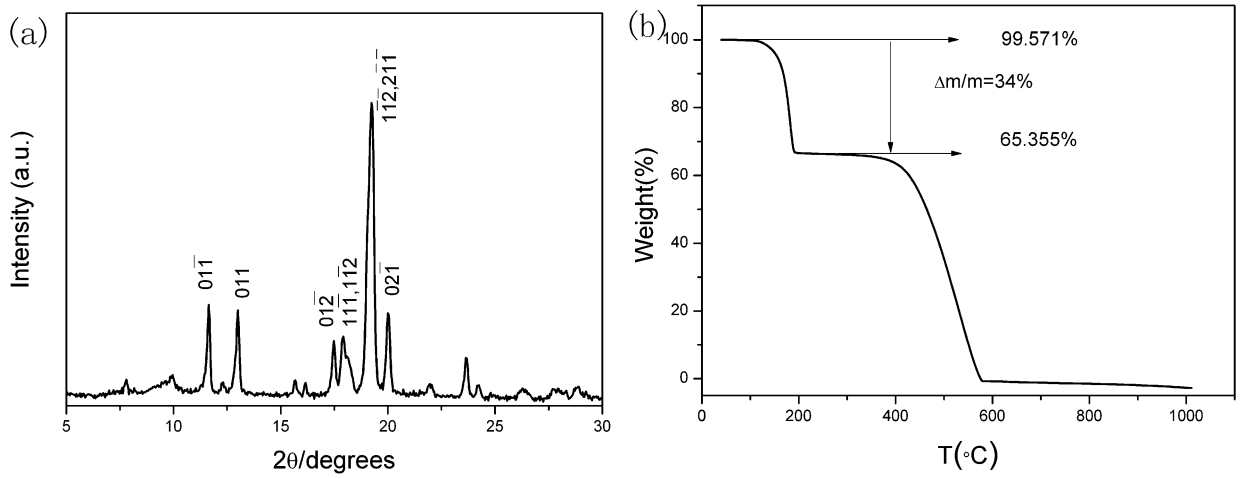

Figure 2. XRD pattern (a) and TGA curve (b) of $C_{60}(Fc)_2$.

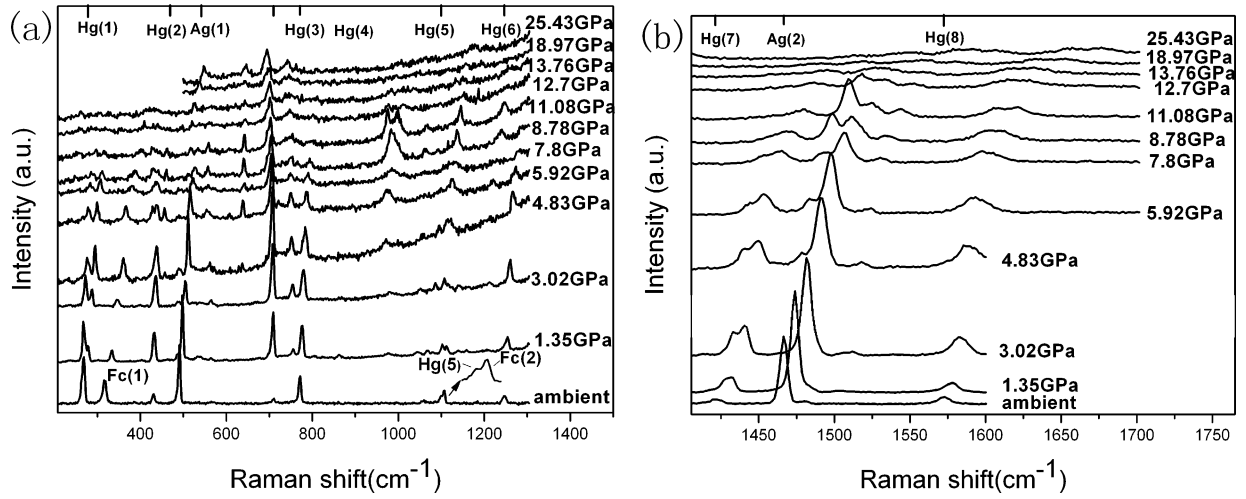

Figure 3. Raman spectra at lower frequency (a) and higher frequency (b) for $C_{60}(Fc)_2$ under different pressures. Ticks at the top indicate the positions of the Raman modes of pure C_{60} at atmospheric pressure.

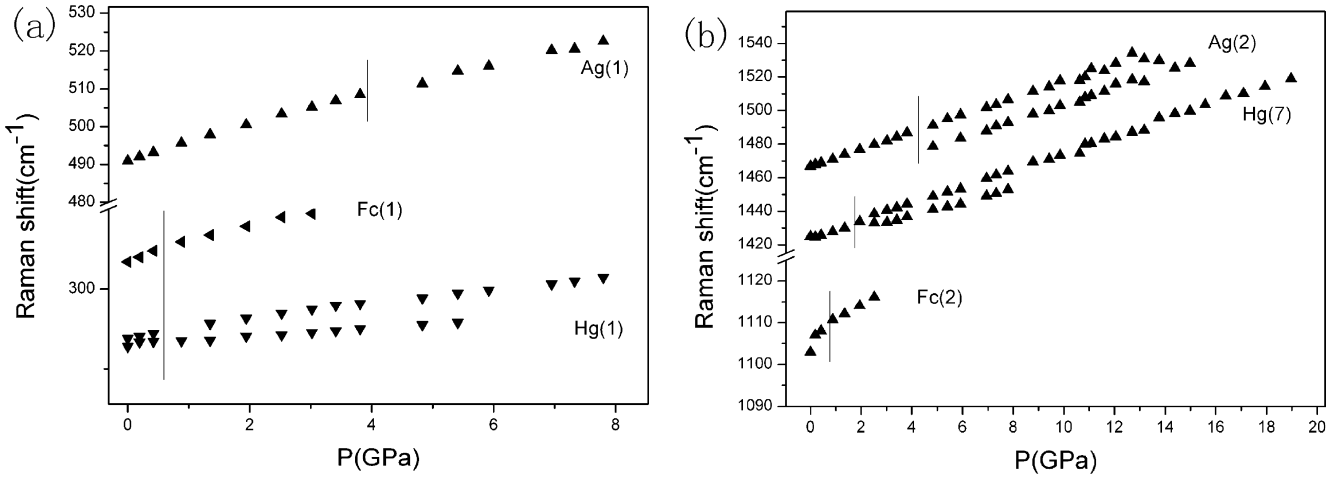

Figure 4. Pressure evolution of the low-frequency (a) and high-frequency (b) Raman modes. The vertical solid lines indicate the domains where the pressure-induced changes are established.

transition from the fcc structure to a less compressible simple cubic (sc) structure due to the orientational ordering of C_{60} molecules in pure C_{60} (nano)crystals.[24] However, we have not observed any change in the pressure dependence slope of other Hg and Ag modes, which suggests that this transition cannot be caused by the orientational phase transition. Based on the difference from pure C_{60}, we propose that such a transition in the Raman modes may be attributed to an enhancement of the

dx.doi.org/10.1021/jp210712y | J. Phys. Chem. B 2012, 116, 2643–2650

Table 1. Observed Pressure Dependences of the Raman Shifts at Room Temperature

	pressure dependences of Raman shift in different pressure ranges (cm^{-1}/GPa)		
modes	0−1.35 GPa	1.35−5 GPa	>5 GPa
$H_g(1)$(267 cm^{-1})	6.62(0.15)	4.19(0.08)	
	0.88(0.07)	2.68(0.09)	–
Ag(1)(490 cm^{-1})	4.59(0.07)		3.58(0.04)
$H_g(7)$(1422 cm^{-1})		5.04(0.04)	
	–	3.89(0.11)	–
Ag(2)(1467 cm^{-1})		5.06(0.06)	
	–	–	5.02(0.1)
Fc(1)(317 cm^{-1})	12.47(0.88)	6.91(0.29)	–
Fc(2)(1105 cm^{-1})	5.4(0.37)	3.36(0.09)	–

interaction between Fc and C_{60} involving an increased charge transfer, since an obvious splitting in the Hg modes is usually observed in alkali-metal-doped C_{60} with a significant charge transfer between the dopants and the C_{60} molecules.[23] Because the Raman features of the charge transfer effect increase with pressure, we further compare the Raman spectrum of $C_{60}(Fc)_2$ at several selected pressures below 4 GPa with that of the one-charge-transferred alkali-metal-doped fulleride K_1C_{60}[25] in Figure 5. From this figure, we see that as the pressure increases,

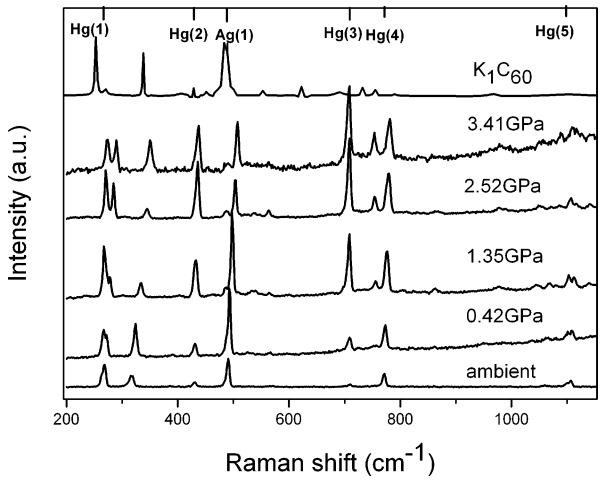

Figure 5. Raman spectra of K1C60 at ambient conditions (top) and C60(Fc)2 at several selected pressures for the low frequency. Ticks at the top indicate the positions of the Raman modes of pristine C_{60} at atmospheric pressure.

the Hg(1) mode shows an obvious splitting and that there are significant changes in the Hg(2) (400−600 cm^{-1}), Hg(3), and Hg(4) (700−800 cm^{-1}) modes. All these Raman modes have features quite similar to those of low value of charge transfer KC_{60}, RbC_{60}, and CsC_{60} polymers[25,26] which have significant changes in most Hg modes compared to that of pristine C_{60}. As we know, the Hg modes of C_{60} are very sensitive to the charge transfer from dopants. The obvious splitting of the Hg modes and the similarities to the behavior of those AC_{60} (A = K, Rb, and Cs) suggest an enhancement in the charge transfer between Fc and C_{60}s. However, the splitting could possibly also be due to a change in the local crystal field on compression.[23]

Regarding the ferrocene modes, the Fc(2) mode softened rapidly and disappeared above ∼3 GPa. In order to explore the possible reason for this, we carried out a high-pressure Raman study on pristine Fc for comparison. In Figure 6 we show the high-pressure Raman spectra recorded from pure Fc. It is

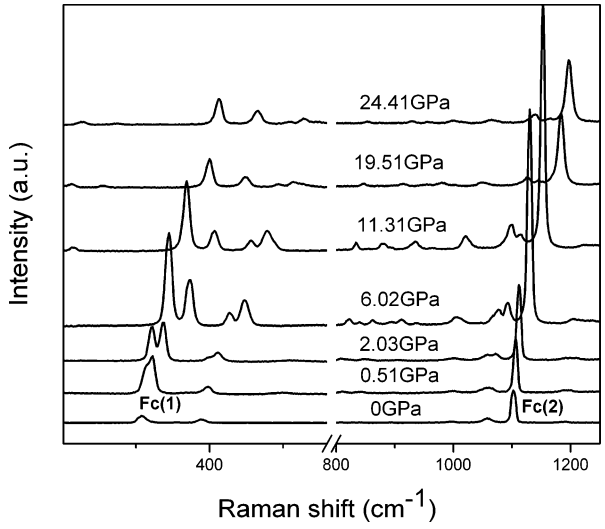

Figure 6. Raman spectra of Fc at high pressures.

observed that some Raman peaks split at low pressure (≤2 GPa) and that most of the Raman modes are very intense even up to 24 GPa. We mainly discuss the Fc(1) and Fc(2) modes here. The Fc(1) mode, which represents the ring−metal stretch,[27] shows a shoulder at very low pressure and splits into two peaks when pressure is increased further, possibly due to some break in symmetry in this stretching mode or an increased interaction among the molecules. In contrast, no splitting is observed for this mode in $C_{60}(Fc)_2$ in the same pressure range, indicating that the ring−metal stretch in our sample is stable up to the highest studied pressure. The Fc(2) mode, which corresponds to ring breathing in Fc,[27] can persist at least up to 24 GPa in pristine Fc, whereas in $C_{60}(Fc)_2$, this mode can hardly be observed above 3 GPa. The unusual softening of this mode is possibly due to an increasing interaction between C_{60} and Fc in $C_{60}(Fc)_2$ under pressure. Thus, this result further supports the suggestion that the interaction between C_{60} and Fc may be strengthened as pressure increases. Adding the similarity with alkali-metal-doped C_{60} mentioned above, we believe the amount of the charge transfer between C_{60}s and Fc can be tuned by applying pressure. This result may be an important key to understand the charge-transfer-induced polymerization in its analogous metal-intercalated fullerides; for example, K-, Rb-, and Cs-doped fullerides A_1C_{60} formed linear polymers between the fulleride ions of the fcc high-temperature phase.[28]

We now turn to a discussion of the changes in the nondegenerate Ag(2) mode of the C_{60} molecules. The position of this mode is a very sensitive probe to detect the formation of polymeric bonds between C_{60} molecules or measure the amount of charge transfer between C_{60} molecules and the intercalated material.[29,30] Relative to pure C_{60}, no shift is observed for the Ag(2) mode of $C_{60}(Fc)_2$ at ambient conditions, indicating that the $C_{60}(Fc)_2$ sample is unpolymerized and suggesting that the charge transfer is small. As described above, at 4.8 GPa the Ag(2) mode displays a shoulder on the lower frequency side, and with increasing pressure the two peaks shift to higher frequency with a constant frequency difference of 12−13 cm^{-1}. It should be noticed that

dx.doi.org/10.1021/jp210712y | J. Phys. Chem. B 2012, 116, 2643−2650

since the Ag(2) mode is nondegenerate, the observation of two peaks implies the simultaneous presence of two different structural phase. The pressure dependence of the higher frequency peak is a smooth continuation of the behavior at lower pressures, and this peak probably still corresponds to undoped molecular C_{60}. The constant extra downshift of the new, second Ag(2) mode can be attributed to a charge transfer effect or the formation of polymeric bonds between C_{60} molecules. However, we also notice the presence of another characteristic feature around 900−1000 cm^{-1} which grows in intensity with increasing pressure. This feature is usually attributed to the presence of a four-membered carbon ring which connects C_{60} molecules by a "2 + 2" cycloaddition mechanism[15] in polymerized C_{60}. Thus, the "splitting" in the Ag(2) mode, i.e., the occurrence of a shoulder at lower frequency, is probably due to the formation of polymeric bonds in parts of the sample, and the downshift of 12−13 cm^{-1} in one of the Ag(2) modes suggests that a linear chainlike polymer structure is formed by the C_{60} molecules.[15,31] This polymerization is also supported by the changes in other vibration modes in the Raman spectra. In Figure 7 we further compare the Raman spectrum from $C_{60}(Fc)_2$ at 4.8 GPa with that from a C_{60} sample in the orthorhombic phase.[32] By a careful comparison, we can clearly see that most of the Hg modes, Ag modes, and the peak at around 960 cm^{-1} characteristic for the polymer bonds have features very similar to those of the one-dimensional chainlike polymer structure of C_{60}. Therefore, all these results suggest that the C_{60} molecules form a chainlike polymer structure in the $C_{60}(Fc)_2$ sample above 4.8 GPa. The Ag(2) mode area always contains vibrational modes from both the chainlike polymerized C_{60} and the starting C_{60}, suggesting that polymerized and unpolymerized C_{60} coexist in the material. The gradual increase in the Ag(2) mode intensity from the polymerized C_{60} with increasing pressure indicates that the C_{60} molecules polymerize progressively into the chainlike polymeric phase, but unpolymerized C_{60} molecules still can be observed close to the highest pressure where all the Raman signals become diffuse. It should also be noted here that the changes in the Raman spectra in our studies are different from those in pristine C_{60} under high pressure, in which case no polymerization (or a random polymerization) is observed at room temperature. In general, it is believed that well-defined one-dimensional C_{60} polymers can only be obtained either by applying simultaneous high-temperature and high-pressure conditions or by doping. Also, in our case there are obvious splits of the Hg(1), Hg(7), and Ag(2) modes, which have never been reported for the high-pressure- and high-temperature-induced C_{60} polymeric structures,[32] indicating a different polymerization result of $C_{60}(Fc)_2$.

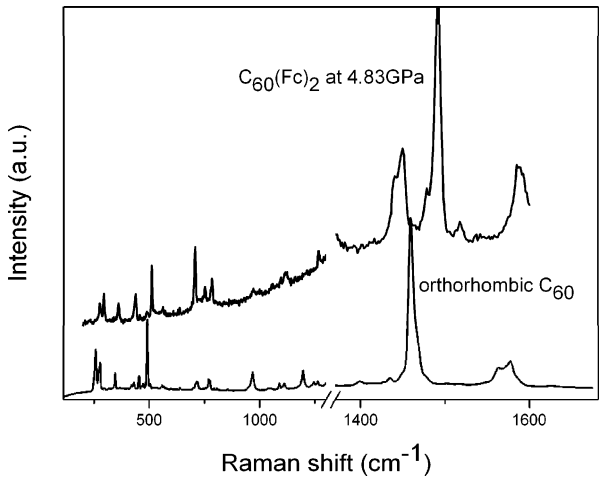

Figure 7. Raman spectra of orthorhombic C_{60} (bottom) and $C_{60}(Fc)_2$ at 4.83 GPa (top).

We have also studied the Raman spectra of the sample during decompression. Figure 8 shows the Ag(2) Raman mode recorded upon compression (a) and decompression (b). The Ag(2) mode is found to return to its starting position of 1467 cm^{-1}. Thus, the polymerization observed under pressure is almost completely reversible.

The reversible polymerization behavior of $C_{60}(Fc)_2$ under pressure is very different from that of pure C_{60}, which is irreversible.[32,33] In previous studies, Zhu et al.[20] observed a reversible polymerization in ternary alkali-metal-doped fulleride under pressure, in which the steric repulsion of the counterions can be overriden at high pressure, resulting in reversible

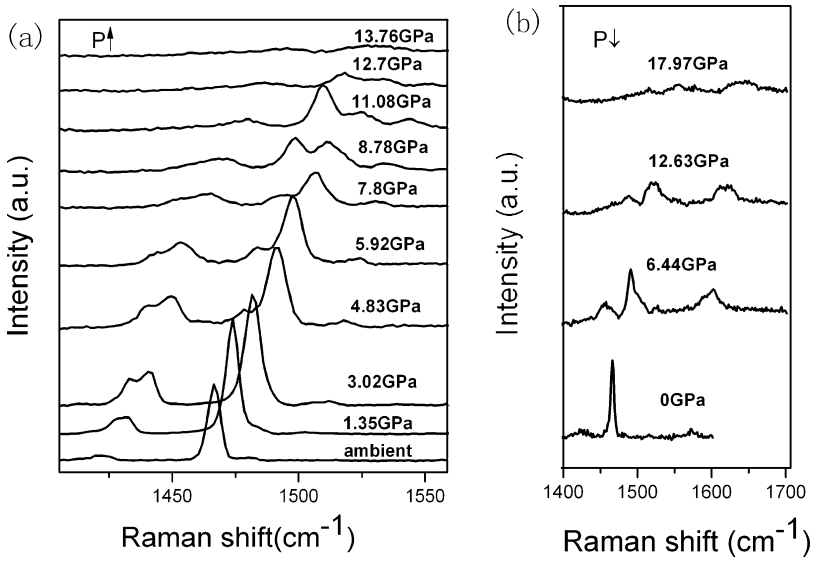

Figure 8. Ag(2) Raman mode for $C_{60}(Fc)_2$ under pressure during (a) compression and (b) decompression.

dx.doi.org/10.1021/jp210712y | J. Phys. Chem. B 2012, 116, 2643−2650

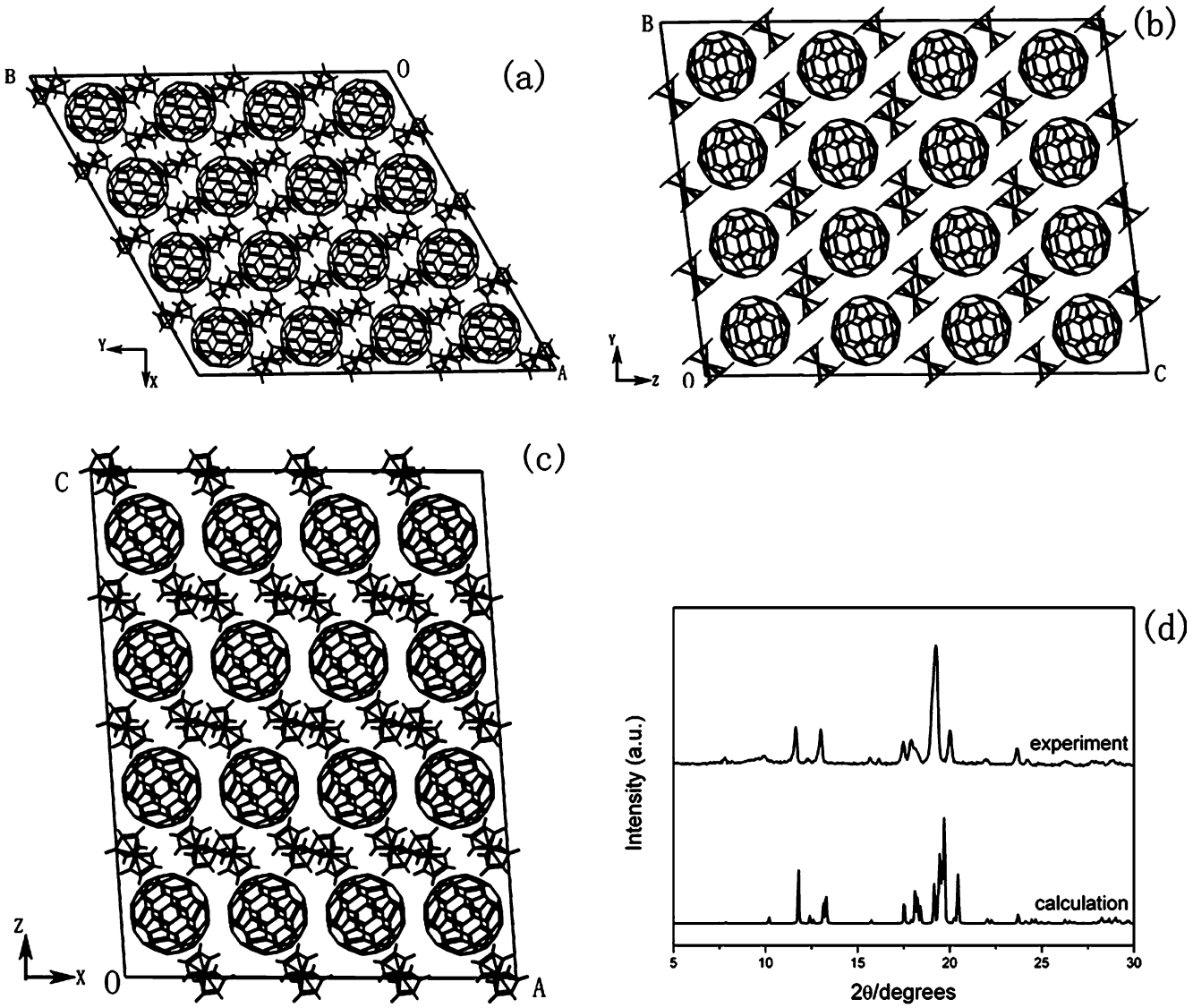

Figure 9. Packing arrangement for $C_{60}(Fc)_2$ in the *ba* plane (a), *bc* plane (b), and *ca* plane (c), respectively. (d) XRD pattern of $C_{60}(Fc)_2$ from experiment (top) and calculation (bottom).

polymerization. Yao et al.[34] have also observed a splitting in the Ag(2) mode but an absence of the polymeric Raman feature at 900−1000 cm^{-1} due to a reversible phase separation of Rb_4C_{60} into two nonpolymerized phases under high pressure. We propose that the reversible polymerization observed in our sample is closer to that observed in Na_2RbC_{60} (ref 20) due to the fact that the steric repulsion of counterions can be overridden under high pressure. Therefore, the strengthened charge interaction in $C_{60}(Fc)_2$ may be the key factor that triggers the polymerization of C_{60} at room temperature. This charge interaction with increasing pressure may affect the redistribution of the electron cloud between C_{60} and Fc molecules and thus induce the polymerization of C_{60} molecules. However, the stability of the polymerizaiton is controlled by the steric repulsion of counterions which can be overridden at high pressure and eventually returns to the initial state, leading to the reversible polymerization.

The structure of the linear chainlike polymer formed can be understood from the initial lattice structure of the $C_{60}(Fc)_2$ crystals. The packing arrangements for $C_{60}(Fc)_2$ in different planes calculated by Materials Studio (from data in ref 35) are shown in Figure 9a−c), and the X-ray diffraction profiles from experiment and calculation are compared in Figure 9d. A careful comparison shows that these two XRD patterns are consistent except for a small shift. Thus, the $C_{60}(Fc)_2$ we have studied consists of close-packed layers of C_{60} molecules stacked directly one above the other, parallel to (001) in agreement with a previous report.[35] The layered structure may cause the C_{60} molecules to restrict the vibration of the Fc molecules under pressures, and the geometrical separation of the C_{60} layers prevents the formation of polymeric intercage bonds in the *c* direction. Thus, the polymerization in $C_{60}(Fc)_2$ can only proceed within each layer. Also, both the insufficient reducing of the volume at higher pressures and the competing orientational ordering of C_{60} could be the additional reasons of partial polymerization in our case. These factors, however, should also be related to the existence of Fc molecules in the crystal, for which the interaction between C_{60}s and Fc molecules could affect the rotation and the volume change of C_{60}s under pressure. Therefore, even up to the highest pressure where all C_{60} Raman signals become diffuse, polymerized and unpolymerized C_{60}s are observed to coexist in our study. This is

dx.doi.org/10.1021/jp210712y | J. Phys. Chem. B 2012, 116, 2643−2650

also found in the "complete" polymerization of pristine C_{60}, where unpolymerized region always exist.[31,32,36] The existence of two-dimensional layers of C_{60} molecules separated by ferrocene molecules suggests that either one- or two-dimensional fullerene polymers might, in principle, be created under pressure. The fact that only the one-dimensional (chain) polymer is observed could possibly be a result of the anisotropy of the positions of the ferrocene molecules with respect to the *a* and *b* axes, giving a preferred polymerization direction. However, it is more likely that the chain formation follows from the weak charge transfer. For alkali-metal-doped fullerides, it is known from both experiments and theory[37] that for a charge transfer of up to one electron per molecule the most stable structures are dimers or linear structures bonded by the (2 + 2) cycloaddition mechanism, and it is highly likely that the same applies to the polymers observed in this work.

4. CONCLUSION

In conclusion, high-pressure Raman studies have been carried out on single crystal $C_{60}(Fc)_2$ nanosheets up to 25.4 GPa. Our results show that the charge transfer between Fc and C_{60} molecules is strengthened in the low-pressure range. This is evidenced by a fast softening of the Raman modes of the inserted Fc under pressure compared to the pure Fc, as well as by Raman features in C_{60}, in particular for some Hg modes, similar to those observed in alkali-metal-doped fullerides. Above 5 GPa the C_{60} molecules start to gradually form polymer chains with increasing pressure. Only certain C_{60} molecules can take part in this reaction, and the polymerization can only proceed within single layers due to the special layered structure in the $C_{60}(Fc)_2$ nanosheets, the resulting spatial restriction, the possible insufficient reducing of the volume, and competing orientational ordering of C_{60}. The observed polymerization is induced by the increased charge transfer under pressure and is found to be reversible upon decompression, which are quite different from what is observed for pure C_{60}. The reversibility of the polymerization is probably due to the overridden steric repulsion of counterions at high pressure.

AUTHOR INFORMATION

Corresponding Author

*E-mail: liubb@jlu.edu.cn. Phone: +00 86 431 85168256. Fax: +00 86 431 85168256.

Notes

The authors declare no competing financial interest.

ACKNOWLEDGMENTS

This work was supported financially by the National Basic Research Program of China (2011CB808200), the NSFC (10979001, 51025206, 51032001, 21073071, 11004072, 11004075, 11104105), and the Cheung Kong Scholars Programme of China. The authors thank Prof. Bertil Sundqvist for useful discussions.

REFERENCES

(1) Haddon, R. C.; Hebard, A. F.; Rosseinsky, M. J.; Murphy, D. W.; Duclos, S. J.; Lyons, K. B.; Miller, B.; Rosamilia, J. M.; Fleming, R. M.; Kortan.; et al. *Nature* **1991**, *350*, 320−321.

(2) Roth, G.; Adelmann, P. *Appl. Phys. A: Mater. Sci. Process.* **1993**, *56*, 169−174.

(3) Konarev, D. V.; Kovalevsky, A. Y.; Khasanov, S. S.; Saito, G.; Lopatin, D. V.; Umrikhin, A. V.; Otsuka, A.; Lyubovskaya, R. N. *Eur. J. Inorg. Chem.* **2006**, *2006*, 1881−1895.

(4) Ma, H. L.; Zhang, X. M.; Liu, B. B.; Li, Q. J.; Zeng, Q. F.; Yu, S. D.; Zou, B.; Cui, T.; Zou, G. T.; Liu, Z. X.; Wågberg, T.; Sundqvist, B.; Noreus, D. *J. Phys. Chem. Lett.* **2010**, *1*, 714−719.

(5) Kalbáč, M.; Kavan, L.; Zukalová, M.; Dunsch, L. *J. Phys. Chem. B* **2004**, *108*, 6275−6280.

(6) Sharma, H.; Garg, I.; Dharamvir, K.; Jindal, V. K. *J. Phys. Chem. A* **2009**, *113*, 9002−9013.

(7) Li, F. H.; Werner, A.; Pfeiffer, M.; Leo, K.; Liu, X. J. *J. Phys. Chem. B* **2004**, *108*, 17076−17082.

(8) Moriyama, H.; Kobayashi, H.; Kobayashi, A.; Watanabe, T. *Chem. Phys. Lett.* **1995**, *238*, 116−121.

(9) Konarev, D. V.; Lyubovskaya, R. N.; Drichko, N. V.; Yudanva, E. I.; Shul'ga, Y. M.; Litvinov, A. L.; Semkin, V. N.; Tarasov, B. P. *J. Mater. Chem.* **2000**, *10*, 803−818.

(10) Wakahara, T.; Sathish, M.; Miyazawa, K.; Hu, C.; Tateyama, Y.; Nemoto, Y.; Sasaki, T.; Ito, O. *J. Am. Chem. Soc.* **2009**, *131*, 9940−9944.

(11) Liu, D. D.; Yao, M. G.; Wang, L.; Li, Q. J.; Cui, W.; Liu, B.; Liu, R.; Zou, B.; Cui, T.; Liu, B. B.; Liu, J.; Sundqvist, B.; Wågberg, T. *J. Phys. Chem. C* **2011**, *115*, 8918−8922.

(12) Yao, M. G.; Liu, B. B.; Zou, Y. G.; Wang, L.; Cui, T.; Zou, G. T.; Li, J. X.; Sundqvist, B. *J. Phys. Chem. B* **2006**, *110*, 15284−15290.

(13) Li, Z. P.; Liu, B. B.; Yu, S. D.; Wang, J. H.; Li, Q. J.; Zou, B.; Cui, T.; Liu, Z. X.; Chen, Z. Q.; Liu, J. *J. Phys. Chem. C* **2011**, *115*, 357−361.

(14) Nagel, P.; Pasler, V.; Lebedkin, S.; Soldatov, A.; Meingast, C.; Sundqvist, B.; Persson, P.-A.; Tanaka, T.; Komatsu, K.; Buga, S.; Inaba, A. *Phys. Rev. B* **1999**, *60*, 16920−16927.

(15) Sundqvist, B. *Adv. Phys.* **1999**, *48*, 1−134.

(16) Blank, V. D.; Buga, S. G.; Serebryanaya, N .R.; Dubitsky, G. A.; Sulyanov, S. N.; Popov, M. Yu.; Denisov, V. N.; Ivlev, A. N.; Mavrin, B. N. *Phys. Lett. A* **1996**, *220*, 149−157.

(17) San-Miguel, A. *Chem. Soc. Rev.* **2006**, *35*, 876−889.

(18) Wang, L.; Liu, B. B.; Liu, D. D; Yao, M. G.; Yu, S. D.; Hou, Y. Y.; Zou, B.; Cui, T.; Zou, G, T.; Sundqvist, B.; Luo, Z. J.; Li, H.; Li, Y. C.; Liu, J.; Chen, S. J.; Wang, G. R.; Liu, Y. C. *Appl. Phys. Lett.* **2007**, *91*, 103112−103114.

(19) Wågberg, T.; Stenmark, P.; Sundqvist, B. *J. Phys. Chem. Solids* **2004**, *65*, 317−320.

(20) Zhu, Q. *Phys. Rev. B* **1995**, *52*, R723−R726.

(21) Talyzin, A. V.; Dubrovinsky, L. S.; Jansson, U. *Solid State Commun.* **2002**, *123*, 93−96.

(22) Espeau, P.; Barrio, M.; Lopez, D. O.; Tamarit, J. L.; Ceolin, R.; Allouchi, H.; Agafonov, V.; Masin, F.; Szwarc, H. *Chem. Mater.* **2002**, *14*, 321−326.

(23) Zhou, P.; Wang, K. A.; Wang, Y.; Ecklund, P. C.; Dresselhaus, M. S.; Dresselhaus, G.; Jishi, R. A. *Phys. Rev. B* **1992**, *46*, 2595−2605.

(24) Snoke, D. W.; Raptis, Y. S.; Syassen, K. *Phys. Rev. B* **1992**, *45*, 14419−14422.

(25) Winter, J.; Kuzmany, H. *Phys. Rev. B* **1995**, *52*, 7115−7123.

(26) Bormann, D.; Sauvajol, J. L.; Goze, C.; Rachdi, F. *Phys. Rev. B* **1996**, *54*, 14139−14145.

(27) Bodenheimer, J.; Loewenthal, E.; Low, W. *Chem. Phys. Lett.* **1969**, *3*, 715−716.

(28) Pekker, S.; Forro, L.; Mihaly, L.; Janossy, A. *Solid State Commun.* **1994**, *90*, 349−352.

(29) Xu, C. H.; Scuseria, G. E. *Phys. Rev. Lett.* **1995**, *74*, 274−277.

(30) Bellin, Ch.; Chervin, J. C.; Hérold, C.; Bendiab, N. *Phys. Rev. B* **2008**, *77*, 245409(6).

(31) Wågberg, T.; Jacobsson, P.; Sundqvist, B. *Phys. Rev. B* **1999**, *60*, 4535−4538.

(32) Wågberg, T.; Soldatov, A.; Sundqvist, B. *Eur. Phys. J. B* **2006**, *49*, 59−65.

(33) Davydov, V. A.; Kashevarova, L. S.; Rakhmanina, A. V. *Phys. Rev. B* **2000**, *61*, 11936−11945.

(34) Yao, M. G.; Sundqvist, B.; Wågberg, T. *Phys. Rev. B* **2009**, *79*, 081403(R).
(35) Crane, J. D.; Hitchcock, P. B.; Kroto, H. W.; Taylor, R.; Walton, D. R. M. *J. Chem. Soc., Chem. Commun.* **1992**, 1764−1765.
(36) Wågberg, T.; Persson, P. A.; Sundqvist, B. *J. Phys. Chem. Solids* **1999**, *60*, 1989−1994.
(37) Pekker, S.; Oszlányi, G. *Synth. Met.* **1999**, *103*, 2411−2414.